Supporting Information

Thin film oxide-ion conducting electrolyte for near room temperature applications

Iñigo Garbayo,[a,d] Francesco Chiabrera,[a] Nerea Alayo,[a] José Santiso,[b] Alex Morata[a] and Albert Tarancón[a,c,]*

[a] Department of Advanced Materials for Energy Applications, Catalonia Institute for Energy Research (IREC), Jardins de les Dones de Negre 1, 08930 Sant Adrià del Besòs, Barcelona, Spain.

[b] Catalan Institute of Nanoscience and Nanotechnology (ICN2), CSIC, Barcelona Institute of Science and Technology, Campus UAB, Bellaterra, Barcelona, 08193, Spain.

[c] ICREA, Passeig Lluís Companys 23, 08010, Barcelona, Spain.

[d] Present address: CIC Energigune, Parque Tecnológico de Álava, 01510 Vitoria-Gasteiz, Spain.

* atarancon@irec.cat

S1. The effect of pressure and target-to-substrate distance in the deposition of BICUVOX polycrystalline films

Complementary to the set of BICUVOX thin films presented in the main text (deposited at a target-to-substrate distance of d = 11 cm), an additional set of films was prepared at d = 9 cm and varying background oxygen pressures. **Figure S1** shows top view SEM images of the films as a function of pressure. In general, all the films presented high density and good uniformity, similar to the samples deposited at d = 11 cm (see **Figure 1b-g** of the main text). EDX analysis (**Figure S2**) brought similar conclusions as those commented in the main text for the other film series, *viz.* huge variability in the Bi/V ratio when changing background pressure. Bi deficient films were obtained in a first low pressure region A (p < 0.0267 mbar), while Bi rich compositions were measured in a higher pressure region C, p > 0.0267. Stoichiometric films were obtained in the intermediate pressure region B, p ≈ 0.0267 mbar. Unlike the films deposited at d = 11 cm, we did not observe the appearance of a fourth region D at higher pressures where the stoichiometric transfer was recovered.

Interestingly, all the films fell in the same trend when plotted as a function of background oxygen pressure times target-to-substrate distance, $p·d$ (see **Figure S2b**). In this figure, we collected the data from the two set of samples, at d = 9 cm and d = 11 cm with varying background pressure, and we added two extra points at d = 10 cm and d = 12 cm to confirm the goodness of the hypothesis. Again, we can differentiate here four $p·d$ regions (A – D) where films presented either a certain cation deficiency (Bi deficiency at low $p·d$, V deficiency at intermediate $p·d$) or a good stoichiometry transfer ($p·d$ ≈ 0.25 mbar·cm and $p·d$ > 2.75 mbar·cm). Notably, a huge variability on the Bi/V ratio was observed, ranging from Bi/V ≈ 1 (*i.e.* heavily Bi deficient as compared to the ideal stoichiometric transfer, Bi/V = 2.22) to Bi/V ≈ 5 (*viz.* huge V deficiency).

The single trend observed in **Figure S2b** for different target-to-substrate distances confirms the hypothesis that the thin film composition is mainly dominated by plume dynamics, as explained in the main text. Indeed, the scattering events of the plasma species with the background gas are dependent on both the pressure in the chamber and the distance travelled as the plume expands towards the substrate. This is particularly marked at high pressure, where the diffusive deposition regime starts to take place (regions C – D).
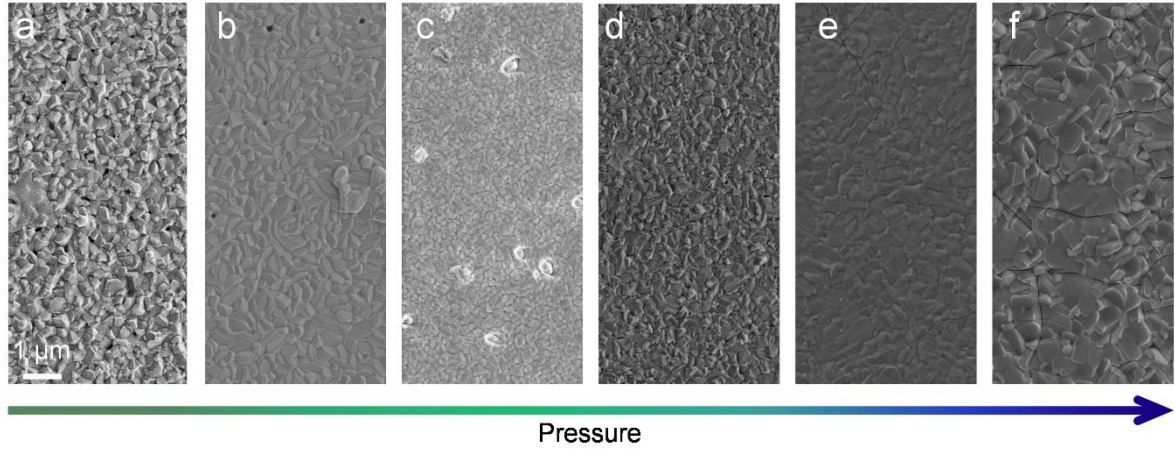
Figure S1. *Top view SEM images of BICUVOX films deposited by PLD at different background pressures and a constant target-to-substrate distance of 9 cm, on top of Si-based substrates. (a) p = 0.0067 mbar, (b) p = 0.0267 mbar, (c) p = 0.0799 mbar, (d) p = 0.133 mbar, (e) p = 0.187 mbar and (f) p = 0.267 mbar.*
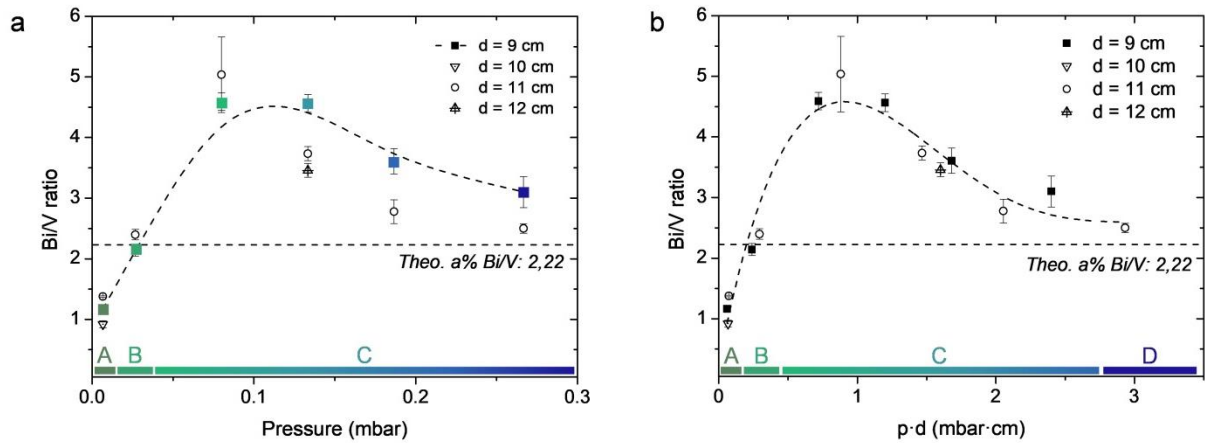

Figure S2. *(a) Bi/V ratio in PLD-deposited BICUVOX films as a function of deposition pressure, at a target-to-substrate distance of 9 cm (coloured squares) and compared to other distances. The figure includes data points from Figure 1(h) (d = 11 cm) and two additional points at distances d = 10 and 12 cm, respectively. Dashed line is included as guide for the eyes. Three different pressure regions are identified for d = 9 cm (A − C, indicated in the figure). (b) Bi/V ratio versus p·d (background oxygen pressure times target-to-substrate distance) in PLD-deposited BICUVOX films.*

Figure S3 shows the appearance of micrometre-size particles on top of the BICUVOX films, when depositing at $p \leq 0.0267$ mbar and independently of the target-to-substrate distance. These particles were found to be Cu-rich when measured by EDX, thus we speculate that they are composed of CuO and coming from the Cu not incorporated in the thin film.
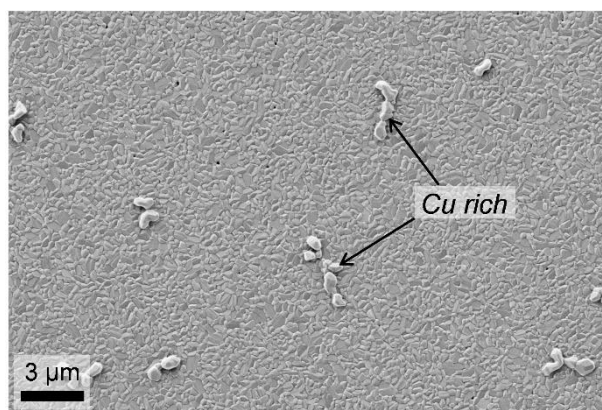

Figure S3. *Top view SEM image of a BICUVOX film deposited at* p *= 0.0267 mbar and* d *= 11 cm. The presence of Cu rich particles (measured by EDX) on top of the film is visible.*

S2. X-Ray diffraction of epitaxial BICUVOX films on STO substrates

Epitaxial BICUVOX deposited on undoped STO showed a similar set of reflections as for the Nb-doped STO, corresponding to the (00L) family of planes, see **Figure S4a**. Equally, the RSM performed on this type of sample (**Figure S4b**) revealed good in-plane matching of substrate and film, derived from the very similar in-plane lattice parameters (as commented in the main text).

Interestingly, an additional set of low intensity peaks (at least 10^3 times lower than the main reflections) is observed in both epitaxial films (on Nb:STO and STO, **Figures 2a** and **S4a** respectively). The appearance of these peaks is clearly observable in the high resolution XRD pattern presented in **Figure S5**, corresponding to the (006) reflection of the BICUVOX (see the peak marked as *, appearing at ~40º). The position of this peak and, in general, of all the set of low intensity peaks matches well with the expected positions of the odd (00L) reflections of the BICUVOX (*e.g.* (007) in **Figure S5**). This could be related to small alterations of the material´s symmetry derived from strain or other structural defects, or to second order effects in the crystal due to inelastic scattering.
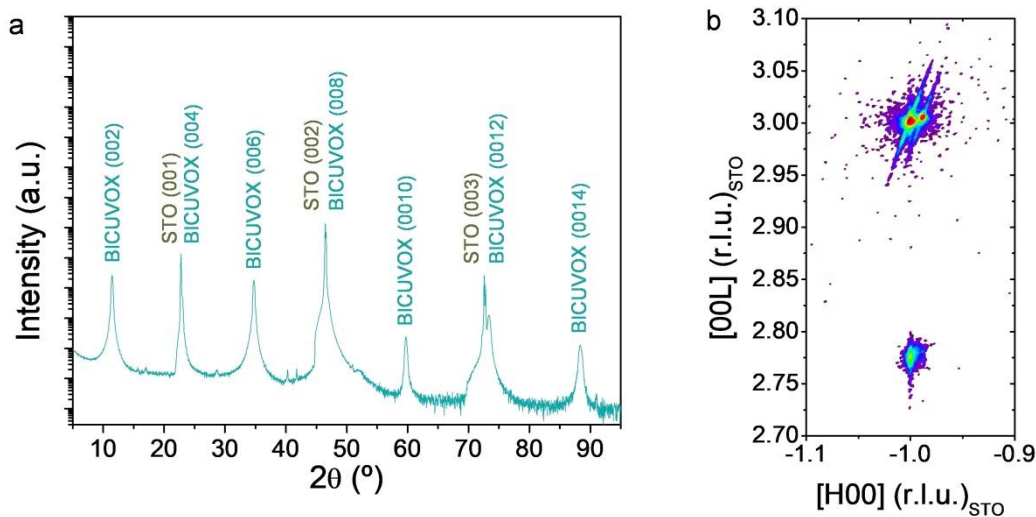

Figure S4. *(a) Out-of-plane ϑ-2ϑ X-Ray Diffraction pattern of a 36 nm thick BICUVOX film deposited on undoped SrTiO₃, where the set of peaks corresponding to the 00L reflexions is visible. (b) In-plane Reciprocal Space Map around the -103 reflexion peak of the SrTiO₃ substrate.*
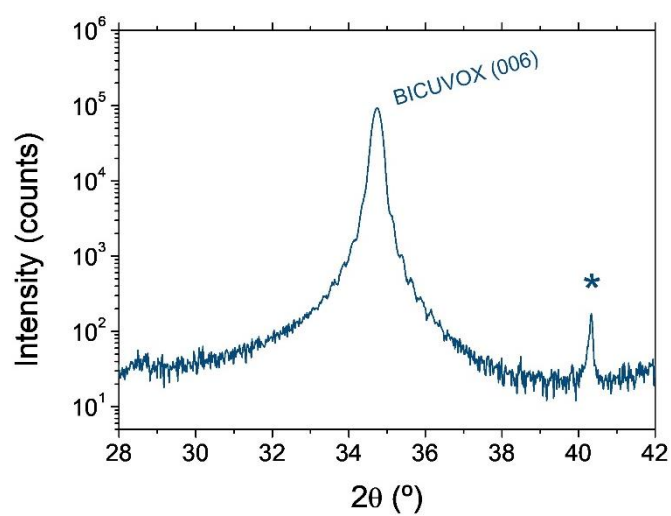
Figure S5. *High resolution out-of-plane ϑ-2ϑ X-Ray Diffraction pattern of a 36 nm thick BICUVOX film deposited on Nb-doped SrTiO₃, focusing on the 006 reflection. The presence of a low intensity peak at ~40º is clearly visible (marked as *).*

S3. Electrochemical Impedance Spectroscopy of polycrystalline and epitaxial BICUVOX films: measuring configurations

Figure S6 collects schematics of the two measuring configurations employed, *viz.* in-plane measurements for polycrystalline (on $Si_3N_4/SiO_2/Si$ substrates) and epitaxial (on undoped STO) films, and cross-plane measurements for epitaxial films (on Nb-doped STO substrates). In all the cases, top Au microelectrodes were defined by photolithography in order to reach short electrode-to-electrode distances (for the in-plane configuration, down to d = 100 μm) or small well-defined circular shapes (for cross-plane, radius from to 50 to 500 μm).

Representative Nyquist plots and distribution of relaxation times (DRT) at selected temperatures are also included in the figure. The DRT were obtained by the MATLAB GUI toolbox developed by Ciucci and coworkers and based on the discretization of the spectra with different Basis Functions.[1] In this work, Gaussian based function was chosen and an analysis on each spectrum collected was conducted to find the best regularization parameters.

In polycrystalline BICUVOX films, three different contributions could be identified, see **Figure S6d** and **S6g**. Two overlapped RQ elements could be differentiated at high-to-medium frequencies, which could presumably be associated to bulk and grain boundary contributions. However, in this type of measurements the stray capacitance determined by the substrate is commonly convoluting all the single contributions from the thin film, making very difficult to distinguish the results in terms of grain and grain boundary contributions. Moreover, in the case of BICUVOX different thin films orientations would determine different bulk conductivities, making challenging the physical interpretation of the two contributions. Therefore, in this study we decided to focus on the total resistance (sum of the two contributions at high-to-medium frequencies). The BICUVOX ionic resistance obtained by equivalent model fitting and by integration of the DRT high frequency peaks[2] was found to be identical. At low frequencies, an additional constant phase element (Q) typical of Au blocking electrodes is observed.
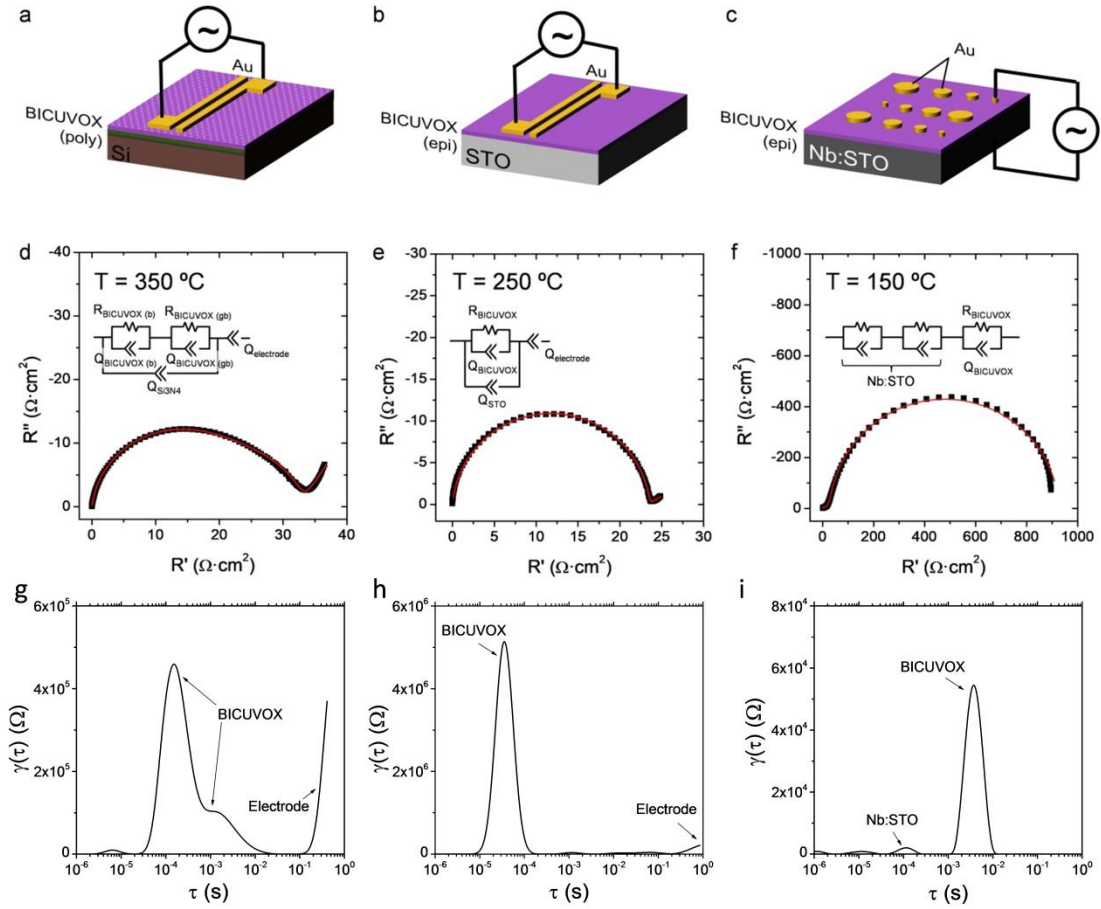
Figure S6. *Measuring configurations and representative Nyquist plots (d-e) and distribution of relaxation times (g-h) for the different types of BICUVOX films: (a,d,g) polycrystalline BICUVOX on top of Si$_3$N$_4$/SiO$_2$/Si (in-plane measurements), (b,e,h) epitaxial BICUVOX on top of undoped STO for in-plane measurements and (c,f,i) epitaxial BICUVOX on top of Nb-doped STO for cross-plane measurements. Black squares correspond to the experimental data measured by EIS and red lines to the fitting. Equivalent circuits are included as insets and measuring temperatures are also indicated.*

In the in-plane measurements of epitaxial films, only one contribution to the BICUVOX ionic conductivity is observed both in the Nyquist plot and in the DRT analysis (**Figure S6e** and **S6h** respectively). Although again the stray capacitance of the STO might play a role masking different contributions, this matches well with the absence of grain boundaries expected for the epitaxial films. It is therefore assumed that this contribution corresponds to the bulk conductivity of BICUVOX. The contribution of the Au blocking electrodes at low frequencies is equally observed in these films. Finally, the cross-plane measurements of epitaxial

BICUVOX films on top of Nb:STO (**Figure S6f** and **S6i**) also shows the presence of one single contribution associated to the film. Additional small contributions are always detected at high frequencies, and are assumed to come from the Nb:STO substrate.

S4. Disambiguation of the substrate effect on the in-plane measurements of BICUVOX films

Regarding the in-plane characterization of the epitaxial films, an additional test has been carried out in order to discard a possible interference of the STO substrate in the measurements, what could lead to a misinterpretation of the results. We measured the in-plane resistance on a bare STO substrate with no film deposited on top, under the same measuring configuration than that used for the BICUVOX films (**Figure S6b**). The bare STO had been previously subjected to the same thermal cycles than the films, *viz.* reproducing the PLD deposition conditions (T = 600 ºC, p = 0.267 mbar). In **Figure S7**, we directly compare the calculated in-plane conductivity of a STO substrate similar to the one used for the deposition of the films with the epitaxial BICUVOX film (from **Figure 3a**). As it can be observed, for temperatures below 300 ºC, more than 4 orders of magnitude lower conductivity was always measured for the STO substrate compared to the films. This corresponds to more than one order of magnitude higher resistance when directly comparing both measurements, thus the measurement error coming from the substrate could be neglected.

Still, the measured conductivity of BICUVOX films on STO could eventually be associated to possible interfacial effects between the film and the substrate and/or element interdiffusion. In order to discard this possibility, an additional film was prepared on a different substrate, in this case the ionic conductor $NdGaO_3$ (NGO). NGO presents an orthorhombic structure that can be alternatively represented according to a pseudo-cubic crystal structure. When oriented (110) (in pseudo-cubic notation), epitaxial BICUVOX could eventually be grown with an in-plane lattice strain of -1.1 % ($a_{NGO,pc}$ = 3.86 Å). **Figure S7** collects as well the measured in-plane conductivity for a BICUVOX film grown on top of NGO, as well as for the bare NGO substrate. As it can be observed, a comparable conductivity was obtained for BICUVOX films grown in the two different substrates, while the NGO substrate presented a conductivity even lower than the STO, at least 5 orders of magnitude below the calculated one for BICUVOX (> 2 orders of magnitude in resistance).

These two measurements led us to conclude that the high in-plane conductivity measured can be undoubtedly associated to the epitaxial BICUVOX films, as described in the main text.

Possible strain effects on the films (*i.e.* comparison between BICUVOX grown on STO and NGO) will be discussed in the future in follow-up work.
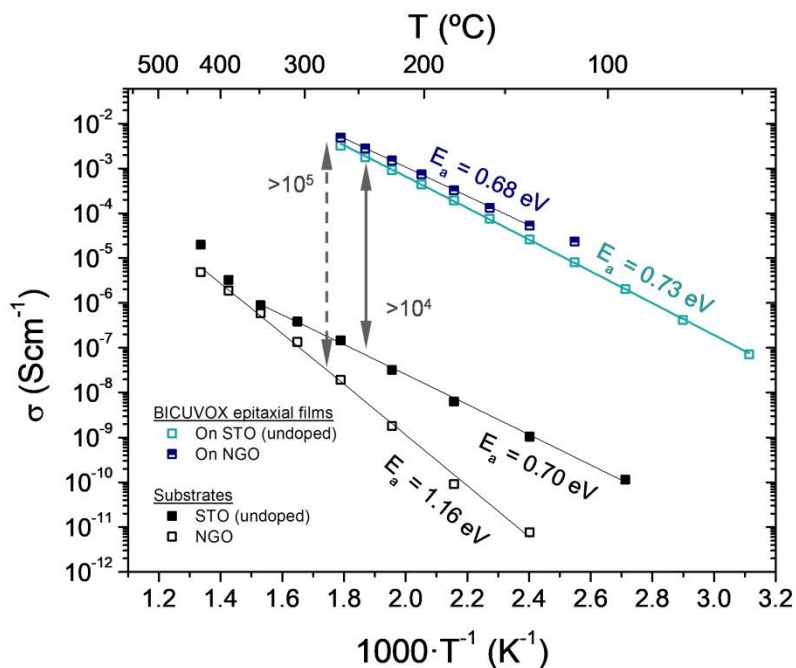

Figure S7. *Arrhenius representation of the evolution of ionic conductivity for BICUVOX epitaxial films with temperature, deposited on two different substrates (STO, NGO). The conductivity measured on the bare substrates under the same measuring configurations is plotted as well, for comparison.*

S5. Ionic conductivity in polycrystalline BICUVOX films as a function of the deposition pressure

Figure S8 presents in an Arrhenius representation the evolution of ionic conductivity of several BICUVOX films, deposited at selected background oxygen pressures (p). In line with the stoichiometric and phase changes observed as a function of p, the highest conductivity is obtained for the films deposited in pressure regions B and D, i.e. where desired stoichiometry is maintained. Intermediate pressures (region C) leads to reduced conduction, probably related to the presence of secondary phases and non-stabilization of the high conducting γ-phase.

Noteworthy, despite obtaining the desired Bi/V ratio, a significant hysteresis is observed in consecutive heating/cooling cycles in the films deposited at p = 0.0267 mbar (note the higher conductivity and lower activation energy obtained in the cooling cycle compared to the heating in **Figure S8**). This hysteresis behavior was proven reproducible during consecutive heating and cooling cycles. Such a behavior has been previously observed for BICUVOX samples with lower concentration of Cu (see reference 51 in the main text), in which the high conducting γ-phase is not stabilized at low temperatures. In those cases, the α-phase is stable at room temperature and a $\alpha \rightarrow \gamma$ transition is expected during heating (see sudden change in activation energies at ~400ºC in **Figure S8**), significantly increasing the ionic conductivity. Although not clearly observed in our case, an additional $\gamma \rightarrow \beta$ transition is expected at high temperatures when starting cooling, remaining the metastable β-phase down to room temperature. We therefore speculate that this behavior is related to the Cu not incorporated in the films, see **Figure S3**, which in this film prevents the stabilization of the high conducting γ-phase in the whole range of temperatures.
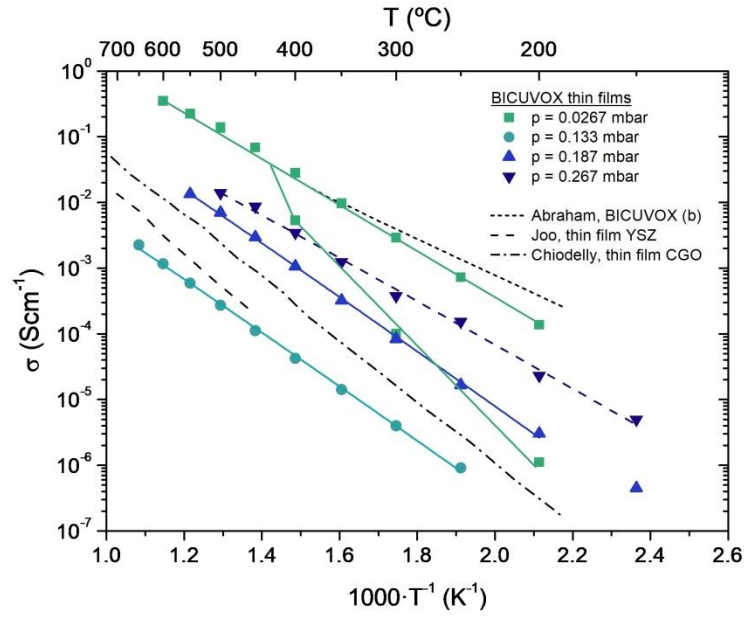
Figure S8. *Arrhenius representation of the evolution of ionic conductivity for different BICUVOX polycrystalline films with temperature, deposited at selected background pressures: p = 0.0267, 0.133, 0.187 and 0.267 mbar. References for bulk polycrystalline BICUVOX and bulk YSZ (references [28], [47] and [49] in the main text, respectively) are included for comparison. Note the two arrows indicating the measurements corresponding to heating and cooling cycles on the film deposited at p = 0.0267 mbar.*

Additional references in the supplementary file

1   T. H. Wan, M. Saccoccio, C. Chen and F. Ciucci, *Electrochim. Acta*, 2015, **184**, 483–499.

2   F. Dion and A. Lasia, *J. Electroanal. Chem.*, 1999, **475**, 28–37.